THE JOURNAL OF BIOLOGICAL CHEMISTRY VOL. 283, NO. 41, pp. 27585–27597, October 10, 2008

Runx2 Regulates G Protein-coupled Signaling Pathways to Control Growth of Osteoblast Progenitors*

Received for publication, March 28, 2008, and in revised form, July 11, 2008 Published, JBC Papers in Press, July 14, 2008, DOI 10.1074/jbc.M802453200

Nadiya M. Teplyuk[‡], Mario Galindo[‡1], Viktor I. Teplyuk[§], Jitesh Pratap[‡], Daniel W. Young[‡2], David Lapointe[‡¶], Amjad Javed[‡3], Janet L. Stein[‡], Jane B. Lian[‡], Gary S. Stein[‡], and Andre J. van Wijnen[‡4]

From the [‡]Department of Cell Biology and Cancer Center, [§]Bioinformatics Core, Program in Molecular Medicine, and [¶]Information Services, University of Massachusetts Medical School, Worcester, Massachusetts 01655

Runt-related transcription factor 2 (Runx2) controls lineage commitment, proliferation, and anabolic functions of osteoblasts as the subnuclear effector of multiple signaling axes (*e.g.* transforming growth factor-β/BMP-SMAD, SRC/YES-YAP, and GROUCHO/TLE). Runx2 levels oscillate during the osteoblast cell cycle with maximal levels in G_1. Here we examined what functions and target genes of Runx2 control osteoblast growth. Forced expression of wild type Runx2 suppresses growth of Runx2$^{-/-}$ osteoprogenitors. Point mutants defective for binding to WW domain or SMAD proteins or the nuclear matrix retain this growth regulatory ability. Hence, key signaling pathways are dispensable for growth control by Runx2. However, mutants defective for DNA binding or C-terminal gene repression/activation functions do not block proliferation. Target gene analysis by Affymetrix expression profiling shows that the C terminus of Runx2 regulates genes involved in G protein-coupled receptor signaling (*e.g. Rgs2, Rgs4, Rgs5, Rgs16, Gpr23, Gpr30, Gpr54, Gpr64,* and *Gna13*). We further examined the function of two genes linked to cAMP signaling as follows: *Gpr30* that is stimulated and *Rgs2* that is down-regulated by Runx2. RNA interference of *Gpr30* and forced expression of *Rgs2* in each case inhibit osteoblast proliferation. Notwithstanding its growth-suppressive potential, our results surprisingly indicate that Runx2 may sensitize cAMP-related G protein-coupled receptor signaling by activating *Gpr30* and repressing *Rgs2* gene expression in osteoblasts to increase responsiveness to mitogenic signals.

Stringent regulation of mesenchymal stem cell renewal and the generation and differentiation of the appropriate number of committed osteoprogenitors are critical for development, remodeling, and repair of bone tissue. Runx2 (Runt-related transcription factor 2) is a critical regulator of bone development by driving osteoblast differentiation and formation of a bone-specific mineralized extracellular matrix (1–4). Runx2 regulates osteoblast growth (5, 6) in part through epigenetic mechanisms (7–9) and the ability of Runx2 to promote a non-proliferative state (*e.g.* senescence or quiescence) (6, 10–12). The first evidence that Runx2 affects bone cell growth was the observation that primary calvarial cells from *Runx2* null mice proliferate faster than corresponding wild type osteoblasts, and reintroduction of Runx2 into *Runx2* null cells restores normal cell growth (5). Several studies indicate that Runx2 control of proliferation is cell type-specific. Runx2 inhibits proliferation of osteoprogenitors and committed osteoblasts (5, 6), but it may have distinct biological roles in chondrocytes (2, 6, 13) and endothelial cells (14, 15), as well as osteosarcoma cells (6, 12), T cell lymphomas (16, 17), and breast cancer (18). In non-osseous cells (*e.g.* T cells), Runx2 has anti-proliferative potential (19) unless c-Myc levels are elevated (17).

The growth regulatory activity of Runx2 is controlled by cell cycle-dependent modulations in its protein levels. Runx2 expression is modulated during the cell cycle at both transcriptional and post-transcriptional levels and maximal in early to mid-G_1 (6, 20, 21). In addition, Runx2 is phosphorylated during the cell cycle by distinct cyclin-Cdk complexes to regulate its activity or stability by a proteasome-dependent mechanism (6, 15, 20, 22, 23). Runx2 expression and activity in osteoblasts are regulated by a large number of growth regulatory factors and external signals, including fibroblast growth factor 2 (24–26), TGFβ[5]/BMP2 (27–31), and PTH (32). Importantly, retention of Runx2 protein on mitotic chromosomes provides an epigenetic memory of its developmental position in the osteogenic lineage (7, 8) and poises Runx2 to control gene expression in early G_1 (21).

Runx2 is a bifunctional transcription factor that mediates the integration of multiple signaling pathways at nuclear matrix-associated subnuclear foci through interactions with a large

* This work was supported, in whole or in part, by National Institutes of Health Grants R01 AR49069 (to A. v. W.) and R01 AR39588, P01 CA82834, and P30 DK32520 (to G. S. S. and J. B. L.). The costs of publication of this article were defrayed in part by the payment of page charges. This article must therefore be hereby marked "*advertisement*" in accordance with 18 U.S.C. Section 1734 solely to indicate this fact.

[1] Present address: Program of Cellular and Molecular Biology, Institute of Biomedical Sciences, Faculty of Medicine, University of Chile, Santiago, Chile.

[2] Present address: Wolf, Greenfield, and Sacks, P.C., 600 Atlantic Ave., Boston, MA 02210.

[3] Present address: Institute of Oral Health Research, School of Dentistry, University of Alabama, Birmingham, AL 32294.

[4] To whom correspondence should be addressed: Dept. of Cell Biology, 55 Lake Ave. North, Worcester, MA 01655-0106. Tel.: 508-856-5625; Fax: 508-856-6800; E-mail: andre.vanwijnen@umassmed.edu.

[5] The abbreviations used are: TGFβ, transforming growth factor-β; GPCR, G protein-coupled receptor; PTH, parathyroid hormone; PKA, cAMP-dependent protein kinase; PKC, protein kinase C; qRT, quantitative reverse transcriptase; GAPDH, glyceraldehyde-3-phosphate dehydrogenase; IRES, internal ribosome entry site; GFP, green fluorescent protein; EGFP, enhanced GFP; α-MEM, minimum Eagle's α-medium; FBS, fetal bovine serum; PBS, phosphate-buffered saline; siRNA, short interfering RNA; FACS, fluorescence-activated cell sorting; MOPS, 4-morpholinepropanesulfonic acid; PMA, phorbol myristate acetate; CREB, cAMP-responsive element-binding protein; BMP, bone morphogenetic protein; Cdk, cyclin-dependent kinase.

cohort of cofactors (>24 partner proteins) that support activation or repression of *Runx2* target genes in osteoblasts (reviewed in Ref. 1 and see Refs. 33–36). For example, Runx2 interacts with GROUCHO/TLE proteins that require the conserved C-terminal VWRPY pentapeptide of Runx2 for gene repression (37). Runx2 transduces TGFβ/BMP2 signaling through direct interactions with SMAD proteins that bind to a composite protein domain ("NMTS/SMID") that mediates transcriptional activation and subnuclear targeting (31, 38). Furthermore, Runx2 interacts with Yes-associated protein (9), a WW domain-containing protein that transduces signals from the SRC/YES family of tyrosine kinases, as well as a growing number of other WW domain-containing proteins (*e.g.* TAZ, SMURF, and SCHNURRI) that all recognize a PPYP motif linked to the NMTS (39–41). Despite the growing number of Runx2 partner proteins that modify or modulate its transcriptional activity, there is limited understanding of the signaling pathways and Runx2 cofactors that control the growth regulatory potential of Runx2 and the downstream expression programs that mediate its cellular functions.

In this study, we have examined how Runx2 regulates growth of osteoblasts using complementation assays with *Runx2* null calvarial osteoprogenitors in which we introduced wild type or mutant Runx2 proteins. Our studies revealed that DNA binding and C-terminal transcriptional functions of Runx2 are essential for cell growth control. Furthermore, our data suggest that Runx2 may regulate G protein-signaling pathways to modify how osteoblasts respond to mitogenic stimuli.

EXPERIMENTAL PROCEDURES

Cell Culture—Immortalized *Runx2* null cells from mouse calvaria were generated in our laboratory from the fetal calvarial region of Runx2 knock-out mice by stable integration of mTERT as described previously (30). *Runx2* null cells were maintained in αMEM supplemented with 10% fetal bovine serum (FBS) (Atlanta Biologicals, Lawrenceville, GA), 30 mM penicillin/streptomycin, and 100 mM L-glutamine at 37 °C and 5% CO_2-humidified atmosphere. Mouse MC3T3 osteoblasts (6) and primary cultures of calvarial cells from wild type and *Runx2* null mice were maintained as described previously (5, 10). Primary cells were expanded in subconfluent culture for three passages before collection and RNA extraction.

Adenovirus Constructs, Infections, and Transfections—Adenoviral vectors containing cDNAs of full-length Runx2, key deletion mutants 1–361 (ΔC) and 1–432 (Δ432), as well as several point mutants R182Q (DNA binding domain mutant) (7), Y433A (YAP-binding mutant) (42), and H426A/T427A/Y428A (SMAD interaction mutant) (31) were each transferred into the AdenoVator™ expression construct (Qbiogene, Irvine, CA) from the corresponding pcDNA expression vectors described in the indicated references from our research group. Viral packaging of the vectors was performed according to the manufacturer's protocol. Virus preparations were purified using a commercial adenovirus purification kit (Promega, Madison, WI).

Cells were plated for infections in 6-well plates (12.5×10^4 cells/well). After 24 h, cells were infected with 100 multiplicities of infection of each virus in 600 μl of αMEM complemented with 1% FBS for 4 h. Upon addition of 400 μl of media containing 1% FBS, cells were incubated for an additional 10 h. Cell numbers were determined at daily intervals during the next 4 days after infection to determine growth curves and to perform expression analyses. Infection efficiencies were assessed by expression of a green fluorescent protein (GFP) under the control of an IRES signal, and images of GFP-expressing cells were taken using a Carl Zeiss fluorescence microscope with a SPOT camera (Diagnostic Instruments, Inc., Sterling Heights, MI).

Quantitative Real Time Reverse Transcriptase-PCR (qRT-PCR) Analysis—Total RNA for qRT-PCR assays was isolated using TRIzol reagent (Invitrogen), subjected to DNase I digestion, and purified using an RNA purification kit (Zymogen, Orange, CA). Aliquots of RNA (1 μg) were used for reverse transcription (first strand cDNA synthesis kit, Invitrogen) with random hexamer primers. Quantitative PCR was performed with commercially available reagents (Power SYBR Green PCR Master Mix, Applied Biosystems, Foster City, CA) using an automated system (Applied Biosystems 7300 Real Time PCR System) with 0.5 pmol/μl of each of the following primers: Runx2 forward, CGA CAG TCC CAA CTT CCT GT, and reverse, CGG TAA CCA CAG TCC CAT CT; Rgs2 forward, GAG GAG AAG CGG GAG AAA AT, and reverse, GCT TTT CTT GCC AGT TTT GG; osteocalcin forward, CTG ACA AAG CCT TCA TGT CCA A, and reverse, GCG CCG GAG TCT GTT CAC TA; Rgs4 forward, TGC CTT TCT CTC CTC GCT AA, and reverse, GCC GAT GTT TCA TGT CCT TT; Gpr30 forward, CCA AGC CTC AAC ACT CAC AC, and reverse, GAA AAC CAG AAG GGT GGA CA; Rgs5 forward, GCC AGC CAA AAT GTG TAA GG, and reverse, AGC AGA GTC TGG CTT CTG GA; Gpr23 forward, CTG GTG CCA GAG TTT GGT TT, and reverse, TTT TCC CAG AGA GCC TGC TA; Rgs16 forward, GCT CCG ATA CTG GGG GTA TT, and reverse, TTC AGC AGC AAA TCG AAA GA; Gpr54 forward, GGT GCT GGG AGA CTT CAT GT, and reverse, ACA TAC CAG CGG TCC ACA CT; Gna13 forward, CCA CCA TCT ACA GCA ACG TG, and reverse, CCA TGG AGC TGG TTT TTG TT; Gpr64 forward, CTG TGG TTG TGT CCA TCG TC, and reverse, CCA CAT TGC TGT TGA TCC AG; osteopontin forward, ACT CCA ATC GTC CCT ACA GTC G, and reverse, TGA GGT CCT CAT CTG TGG CAT; Wnt7b forward, ATG CCC GTG AGA TCA AAA AG, and reverse, CCT GAC ACA CCG TGA CAC TT; Serpin b2 (PAI2) forward, CAA GAT GGT GCT GGT GAA TG, and reverse, GCT CTC ATG CGA GTT CAC AC; Alk Phos forward, TTG TGC GAG AGA AAG AGA GAG A, and reverse, GTT TCA GGG CAT TTT TCA AGG T; p21 forward, TTG CAC TCT GGT GTC TGA GC, and reverse, TCT GCG CTT GGA GTG ATA GA; Mcox forward, ACG AAA TCA ACA ACC CCG TA, and reverse, GGC AGA ACG ACT CGG TTA TC; Hprt forward, CAG GCC AGA CTT TGT TGG AT, and reverse, TTG CGC TCA TCT TAG GCT TT; histone H4 forward, TGA GCT TCC TTC CTA GTT TGC, and reverse, GCT TAG CAC CAC CCT TAC CA; p27 forward, GTG GAC CAA ATG CCT GAC TC, and reverse, TCT GTT GGC CCT TTT GTT TT; cyclin B2 forward, GCC TCT TGC CTG TCT CAG AA, and reverse, GCT GCA TGA CTT CCA GGA CT.

Rodent GAPDH and ribosomal 18 S RNA internal control primers were purchased from Applied Biosystems. The initial

denaturation occurred at 95 °C for 10 min followed by 40 cycles of two-step PCR (95 °C for 15 s denaturation and 60 °C for 1 min synthesis).

Affymetrix Analysis—Total RNA for Affymetrix analysis (and subsequent qRT-PCR validation) was isolated with TRIzol reagent and purified using the RNeasy mini kit (Qiagen). Approximately 1–5 μg of total RNA was used for two strand cDNA synthesis using the Affymetrix cDNA synthesis kit using oligo(dT) primers (Affymetrix, Santa Clara, CA). Following cRNA synthesis, samples were labeled with biotin using the BioArray HighYield RNA transcript labeling kit (Enzo Lifesciences, Farmingdale, NY) and purified with Affymetrix Cleanup Module for cRNA (Affymetrix). Aliquots of the full-length cRNA products (~20 μg) were fragmented using metal-induced hydrolysis at a concentration of 1 μg/μl. The quality of cRNA fragments (35–200 bases) was evaluated in 1% formaldehyde/MOPS gel. Aliquots of fragmented cRNA (12 μg) were used for hybridization with Affymetrix cDNA microarrays ("chips") (Mouse Genome 430 2.0 Array) in hybridization mixture for 16 h at 42 °C in a hybridization oven. After hybridization, chips were washed on an Affymetrix Fluidics Station and stained with solutions containing streptavidin/phycoerythrin solution and goat IgG antibody to amplify the signals of the transcripts. The resulting signals were scanned using an Affymetrix scanner, and numerical files (CEL) were generated from the resulting images. Data processing and sample comparisons were performed using an open source library for statistical analysis (BioConductor library for R environment). In brief, robust multiarray average expression measure as part of the Affy software package was applied to calculate the average value of signals on the arrays (43). Following robust multiarray average background correction, array values were subjected to quantile normalization assuming identical signal distributions in each of the arrays. Statistically significant differences between probe sets were evaluated using Student's t test ($p < 0.05$). Functional annotation of Affymetrix probe sets and gene ontology relationships between groups of co-regulated genes were assessed using the data base for Annotation, Visualization and Integrated Discovery (DAVID 2.0) (44).

Western Blot Analysis—Cell lysates were prepared from cell pellets that were boiled in 100 μl of Direct Lysis buffer (50 mM Tris-HCl, pH 6.8, 2% SDS, 10% glycerol, 12% urea, 25 μM MG132, 100 mM dithiothreitol, and 1× Complete protease inhibitors) (Roche Applied Science). Aliquots of each lysate (5 μl) were separated in 10% SDS-PAGE. Proteins were transferred using semi-wet blotting to nitrocellulose membranes (Millipore, Billerica, MA). Phosphate-buffered saline (PBS: 20 mM phosphate, 150 M NaCl, pH 7.4) with 5% nonfat milk was used for 1 h at room temperature to block nonspecific protein binding. Primary and secondary antibodies were used at 1:2,000 dilutions for 1 h room temperature in PBS, 0.1% Tween (PBST) with 1% milk. Signal was detected with ECL (Western Lighting Chemiluminescence Reagent Plus, PerkinElmer Life Sciences). Runx2-specific mouse monoclonal antibodies were a generous gift of Dr. Yoshiaki Ito (Institute for Molecular and Cellular Biology, Singapore). CDK2 rabbit polyclonal antibody (SC-163) was purchased from a commercial vendor (Santa Cruz Biotechnology, Santa Cruz, CA).

In Situ Immunofluorescence—Immunofluorescence microscopy was performed according to standard procedures (9, 37). For detection of Gpr30 and Rgs2 protein in adenovirus-infected *Runx2* null cells, we applied the following procedure. *Runx2* null cells were plated on gelatin-coated coverslips at 0.6×10^6 cells per 6-well plate. Cells were infected after 24 h with adenovirus vectors expressing wild type Runx2, the Δ361 mutant, or GFP alone. Cells were fixed with 3.8% formaldehyde in PBS for 10 min and permeabilized with 0.25% Triton X-100 in PBS for 20 min. Nonspecific binding was blocked for 20 min with PBSA solution (PBS containing 0.5% bovine serum albumin). Cells were incubated with the following primary antibodies at a 1:250 dilution in PBSA at 4 °C overnight: rabbit polyclonal specific for Gpr30 (Abcam, Ab-12564) and goat polyclonal specific for Rgs2 (Santa Cruz Biotechnology, C18/sc7678).

For Rgs2 and Ki-67 co-staining, MC3T3 cells were plated at ~0.3×10^6 cells per 6-well plate, fixed 36 h after plating, permeabilized, and blocked as described above. Cells were incubated with a mixture of primary antibodies containing a 1:200 dilution of goat polyclonal anti-Rgs2 antibody (SC-7678, Santa Cruz Biotechnology) plus a 1:100 dilution of rabbit polyclonal anti-Ki67 (Abcam, Ab-15580). Dilutions were made in PBSA, and cells were incubated with antibodies for 1 h at 37 °C. Following 4′,6-diamidino-2-phenylindole staining to define the location of the nucleus, immunodetection of proteins of interest was achieved by incubation for 1 h at 37 °C with 1:800 dilutions (in PBSA) of fluorophore-conjugated secondary antibodies: donkey anti-goat IgG 488 (green), donkey anti-goat IgG 596 (red), and donkey anti rabbit 596 (red) (Invitrogen). Fluorescence images were taken on an Axioplan 2 Carl Zeiss fluorescence microscope (Carl Zeiss, Thornwood, NY) with a Hamamatsu C4742-95 digital camera (Hamamatsu, Bridgewater, NJ). Digital images were acquired within the MetaMorph Imaging Series software environment (version 7.1.3) (Molecular Devices, Sunnyvale, CA).

RNA Interference—RNA interference experiments were carried out using commercially available siRNAs. Specific siRNAs for *Gpr30* (RNA ID 262286), *Gpr54* (RNA ID 85872), and *Rgs4* (RNA ID 64271) were purchased from Ambion (Austin, TX) (see Fig. 6), whereas siRNAs for *Rgs2* (catalog number D-040277-01) and *Gpr30* (J-053623-05) were acquired from Dharmacon (On-target plus siRNAs; Dharmacon, Lafayette, CO) (see Fig. 8). Nonsilencing siRNA1 (Ambion) and siCONTROL nontargeting siRNA1 (Dharmacon) were used as negative controls in our experiments as these siRNAs have no discernible off-target effects on cell growth or the gene expression parameters examined in our study.

For siRNA transfections, cells were plated at a density of ~0.6×10^5 cells/well in 6-well plates and transfected in duplicate after 24 h with 50 nM of each siRNA in Opti-MEM using Oligofectamine reagent according to the recommendations of the supplier (Invitrogen). Concentrated complete α-MEM (2.5×) was added 4 h after transfection to obtain final concentrations of 30 mM penicillin/streptomycin, 100 mM L-glutamine, and 10% FBS. Cells were re-plated 24 h after siRNA transfection to prevent contact inhibition. Samples were collected following trypsinization and either counted or fixed for flow cytometry 36 h after re-plating. An expression vector for *Rgs2*

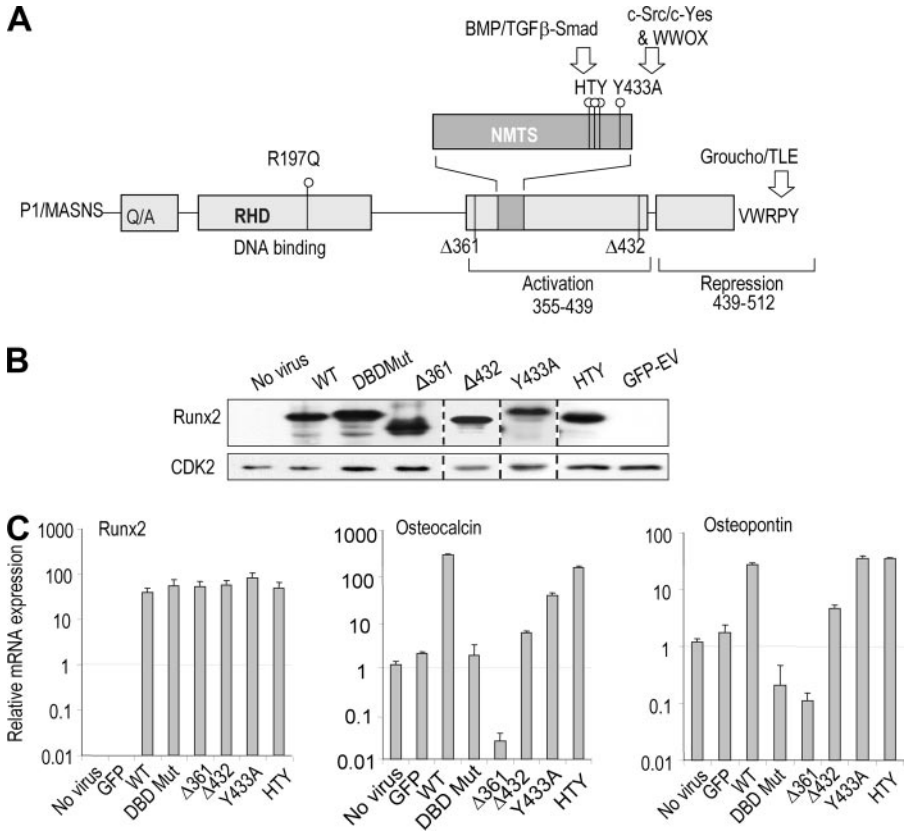

FIGURE 1. **Runx2 reconstitution in osteoprogenitors from *Runx2* null mouse calvaria.** Cells were infected with adenoviral vectors expressing an IRES-driven GFP marker and either Runx2 wild type (*WT*) or different mutants defective for interactions with distinct regulatory cofactors. Virus expressing GFP alone was used as a control (*GFP-EV*). *A,* schematic representation of specific Runx2 mutations used in the context of functional protein domains of Runx2. Numbering is for the P1 isoform of Runx2 that starts with the amino acids MASNS and ends with the conserved residues VWRPY. Also indicated are a poly(Q/A) stretch, the runt homology domain (*RHD*) that controls DNA binding, C-terminal activation, and repression domains, as well as a nuclear matrix targeting signal. Micrographs were taken of transfected cells expressing an IRES-driven GFP at day 2 after infection to establish comparable infection efficiencies of each adenoviral vector (data not shown). *B,* Western blot analysis of exogenous Runx2 protein levels and different mutants shows comparable expression of Runx2 at day 1 after infection. The figure is a representative collage of comparable exposures of four distinct experiments with different sets of adenoviral vectors. Spliced lanes are indicated with *dashed lines*. *C,* expression of Runx2 mRNA levels in *Runx2* null cells and induction of bone marker genes were monitored by qRT-PCR analysis. The mRNA levels for exogenous Runx2 were plotted relative to the average endogenous mRNA level in an equivalent amount of RNA from MC3T3 cells that was examined in parallel as external standard. RNA quantity was normalized relative to GAPDH as internal control. The mRNA levels of osteocalcin and osteopontin in control cells (no virus) are minimal, and values of 1 and below are close to background levels.

(pcDNA3.1-Rgs2) was purchased from University of Missouri Rolla cDNA Resource Center, Rolla, MO. A kanamycin-resistant vector expressing enhanced green fluorescent protein (EGFP) we have used previously (45) was transfected in parallel to evaluate the percentage of transfected cells. For transient DNA transfections, cells were plated in 6-well plates ($\sim 0.6 \times 10^5$ cells/well; same as above for siRNA transfections) and transfected with Lipofectamine (Invitrogen) for 16 h with 0.5 μg of Rgs2 or EGFP-expressing control vector according to protocols from the supplier.

Flow Cytometry—Cells in which the levels of proteins of interest were modulated were examined by fluorescence-activated cell sorting (FACS) to assess the distribution of cells in different cell cycle phases. We performed FACS analysis by trypsinizing cells that were washed with PBS and fixed in 85% ethanol at 4 °C for 24 h. Cells were stained for DNA content with 50 μg/ml propidium iodide in PBS plus 1.8 mM $MgCl_2$ and 50 μg/ml RNase A solution by incubation at 37 °C for 20 min in the absence of light. After the sorting FACS data were analyzed with the Synchronization Wizard module of the ModFit LT 3.0 program (Verity Software House, Topsham, ME).

RESULTS

Runx2 Growth Regulation of Osteoblast Progenitors Requires DNA Binding, as Well as C-terminal Transactivation and Repression Domains—We have previously shown that Runx2 deficiency increases the proliferative potential of osteoprogenitors and that re-introduction of wild type Runx2 into primary calvaria cells restores stringent cell growth control (5). To characterize the mechanisms by which Runx2 controls cell growth, we used deletion and point mutants of Runx2 to assess which functions of Runx2 are required for growth regulation. Wild type and mutant Runx2 proteins (Fig. 1*A*) were expressed from adenoviral vectors that were used to infect immortalized calvarial osteoprogenitors from mice with a homozygous *Runx2* null mutation. Cells were maintained under standard culture conditions without osteogenesis-promoting agents. We achieved >95% infection efficiency for all adenoviral vectors based on fluorescence detection of co-expressed GFP proteins (data not shown), and our set of Runx2 proteins is expressed at comparable levels as assessed by Western blot analysis (Fig. 1*B*) and real time qRT-PCR (Fig. 1*C*). Furthermore, as expected, exogenous expression of wild type Runx2, but not a subset of Runx2 mutants, increases bone phenotypic markers (*e.g.* osteocalcin and osteopontin) (Fig. 1*C*). Re-introduction of wild type Runx2 into *Runx2* null cells inhibits osteoblast proliferation as reflected by a prominent decrease in the slope of the growth curve when compared with control cells expressing GFP alone (Fig. 2, *left*), consistent with our previous observations (5, 6). We note that the inhibitory effects of Runx2 are reversible and that osteoblasts resume proliferation after a delay when transiently expressed Runx2 levels decrease (6).

We tested three different point mutations of Runx2 affecting specific known signaling functions of the protein. We have shown that the C terminus of Runx2 is multifunctional and, for example, integrates BMP/TGFβ signaling, supports nuclear matrix targeting, as well as mediates signaling by WW domain

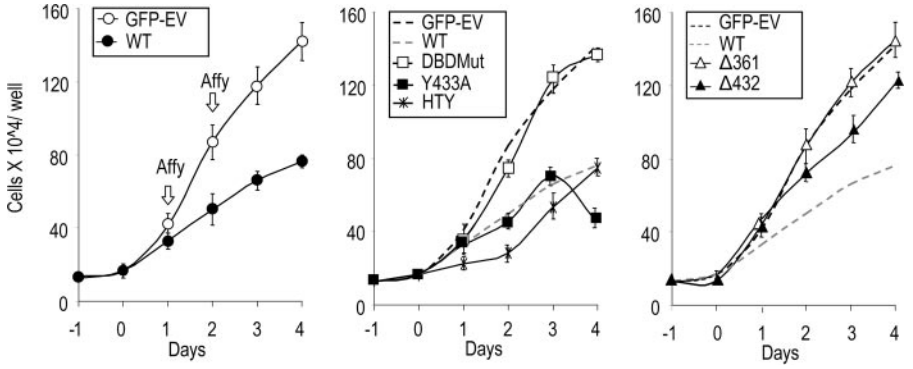

FIGURE 2. **Runx2 growth control in *Runx2* null osteoblasts progenitors requires C-terminal transcriptional activities and DNA binding of Runx2.** Immortalized *Runx2* null cells were infected with adenoviral vectors expressing wild type (*WT*) or mutant Runx2 (plus GFP), or GFP alone at comparable efficiencies of infection as described in Fig. 1. Growth curves were obtained by cell counting at daily intervals until 4 days after infection. Day −1 is the day of plating and day 0 is the day of infection. *Error bars* reflect variation observed in duplicate or triplicate independent experiments. *Left, Runx2* null cells expressing wild type Runx2 (*closed circles*) grow slower than cells transfected with the corresponding empty vector (*open circles*). *Middle,* expression of Runx2 C-terminal point mutants (Yap interaction mutant Y433A (*closed diamonds*) and Smad/nuclear matrix interaction mutant HTY426–428AAA (*dashed crosses*)) results in similar growth inhibition as observed for wild type Runx2. A point mutation that abrogates Runx2 DNA binding activity (R197Q) (*open diamonds*) abrogates the growth inhibitory potential of Runx2. Growth curves for wild type Runx2 (*dashed gray line*) and empty vector (*dashed black line*) were taken from *left panel* and are shown for comparison. *Right,* expression of the C-terminal truncated Runx2 protein Δ361 (*open triangles*) does not inhibit growth, whereas Δ432 (*closed triangles*) exhibits a moderate growth inhibition phenotype compared with wild type Runx2 and empty vector (*dashed lines* taken from *left panel*).

proteins (*e.g.* c-SRC/YES signaling and WOXX signaling) and GROUCHO/TLE-dependent transcriptional repression (1). Because we considered it plausible that each of these functions could be directly linked to control of bone cell proliferation, we focused on mutants with defects in the C terminus of Runx2 (Fig. 1*A*). One Runx2 mutant ("HTY") has a triple amino acid substitution (H426A/T427A/Y428A) that abrogates subnuclear targeting and blocks the interaction of BMP/TGFβ-responsive SMAD proteins with Runx2 (31, 38). The HTY protein blocks cell proliferation (Fig. 2, *middle*) indicating that the BMP/TGFβ-SMAD signaling pathway is dispensable for Runx2 growth regulation.

The second mutant ("Y433A") has a single tyrosine mutation that blocks binding of WW domain proteins, including the YES-associated protein (YAP), which transduces signaling by YES/C-SRC tyrosine kinase pathways (9). Expression of the mutant Y433A Runx2 protein also rescued the hyper-proliferative phenotype of *Runx2* null cells (Fig. 2, *middle*) establishing that YES/C-SRC signaling is not required for growth inhibition. In contrast, the third point mutant ("R197Q") (7) abrogates the DNA binding activity of Runx2 and thus recognition of target gene promoters. Expression of the mutant R197Q protein did not inhibit cell proliferation, and the growth curve for this mutant was indistinguishable from those obtained for control cells infected with the empty vector (Fig. 2, *middle*). Taken together, these data show that DNA binding is essential for the growth regulatory function of Runx2.

To define a specific region of Runx2 that reduces cell growth potential, we tested several C-terminal deletion mutants. One mutant ("Δ361") lacks amino acids 362–528 that encompass distinct transcriptional activation and repression domains. Another deletion mutant lacks amino acids 433–528 ("Δ432") that retains trans-activation potential but does not have a C-terminal repression module. The results show that expression of the Δ361 mutant does not impede proliferation of *Runx2* null cells, demonstrating that the removal of key transcriptional functions renders Runx2 ineffective (Fig. 2, *right*). Expression of the Δ432 deletion mutant appears to suppress cell proliferation but only to a limited degree (Fig. 2, *right*). This intermediate growth inhibitory phenotype suggests that gene repression and trans-activation by Runx2 may each contribute to control of cell proliferation.

Identification of Runx2-responsive Genes That Contribute to Cell Growth Regulation—We used gene expression profiling to assess what genes respond to the re-introduction of Runx2 into *Runx2* null calvarial progenitors during growth inhibition. As above, reconstitution experiments were performed by introducing wild type Runx2 or the Δ361 deletion mutant that does not inhibit cell growth into *Runx2* null cells using adenoviral vectors. Control cells were infected with a vector expressing GFP.

The advantage of our experimental design is that it permits delineation of the effects of Runx2 mutations in the absence of endogenous wild type Runx2 expression. Furthermore, it enables us to detect induction of gene expression by *Runx2* in cells that have not yet biologically activated *Runx2*-responsive genes as a consequence of developing into maturing osteoblasts; the latter is not possible with alternative strategies involving RNA interference with Runx2 siRNA or forced expression of the Δ361 deletion mutant as a competitive inhibitor of wild type Runx2 function.

RNA samples were prepared in triplicate after induction of exogenous *Runx2* gene expression at a time when growth suppression is initiated (day 1) or overtly evident (day 2) (see Fig. 2, *left*). Samples from two independent experiments were subjected to gene expression profiling using Affymetrix mouse cDNA micro-arrays (Fig. 3). Validation of expression values was performed using qRT-PCR with the same samples and new replicates (see Fig. 4). Consistent with expression results for *Runx2* and bone marker genes (see Fig. 1*C*), we observed that Affymetrix expression values for exogenous Runx2 mRNA are robust in cells producing the wild type and the Δ361 deletion mutant but not in GFP-expressing cells (data not shown).

Because growth suppression requires the C terminus of Runx2, we focused our analysis on genes that are preferentially modulated (*i.e.* activated or repressed) by the wild type but not the mutant Δ361 Runx2 protein. We calculated expression ratios for genes modulated by the wild type or Δ361 mutant proteins. Genes were rank ordered based on a statistically significant ($p < 0.05$) fold increase or decrease in their expression. By comparing expression patterns observed for the wild type and Δ361 Runx2 proteins, our data were filtered to eliminate

A

Gene symbol	Description	Known Target	Relative to Δ361,day1	Relative to Δ361, day2	Relative to GFP, day1	Relative to GFP, day 2
Up-regulated by Runx2 wild type vs Runx2 ΔC						
Spp1	Secreted phosphoprotein 1 (osteopontin)	Yes	23.1	4.0	13.6	4.3
Bglap2	Bone gamma-carboxyglutamate protein 2 (osteocalcin)	Yes	6.3	9.0	7.7	10.7
Mmp13	Matrix metalloproteinase 13	Yes	6.2	8.7	7.8	11.2
Timp3	Tissue inhibitor of matrix metalloproteinase 3	-	5.6	3.6	5.0	3.8
Tspan 32	Tetraspanin 32	-	2.6	3.9	2.8	4.1
Gpr30	G-protein coupled receptor 30	-	2.6	2.0	3.1	2.2
Col6a2	Procollagen, type VI, alpha 2	-	2.0	2.4	2.7	2.1
Gpr54	G-protein coupled receptor 54	-	1.5	1.2	1.8	1.2
Down-regulated by Runx2 wild type vs Runx2 ΔC						
Serpinb2	Serine/cysteine proteinase inhibitor b2 (PAI2)	-	8.9	7.9	8.6	5.5
Glyat	Glycine-N-acyltransferase	-	5.5	4.0	7.0	3.8
Rgs2	Regulator of G-protein coupled signaling 2	Yes	4.2	3.7	4.1	3.5
Rgs4	Regulator of G-protein coupled signaling 4	-	2.8	1.4	3.2	1.7
Rgs5	Regulator of G-protein coupled signaling 5	-	2.7	3.5	2.9	4.0
Gpr64	G-protein coupled receptor 64	-	2.6	1.8	2.7	2.3
Rgs 16	Regulator of G-protein coupled signaling 16	-	2.3	2.6	2.0	2.6
Casp4	Caspase 4	-	1.6	3.8	1.9	3.2
Gpr23	G-protein coupled receptor 23	-	1.2	2.8	1.5	1.5

B

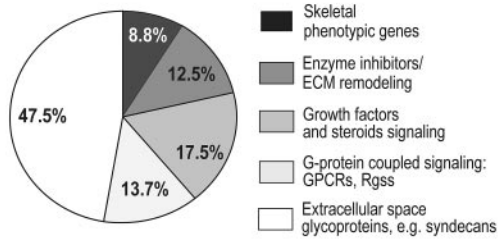

C

Ligands	IL6, IL24, IL33, IL13ra1, Cxcl1, Cxcl5, Cxcl12, Ccl2, Ccl7
Receptors	Gpr30, Gpr54, Gpr23, Gpr64, Gpr124, Npr3, Edg1, Edg5, P2ry6
G-proteins	Gna13, Gnaq, Gnb5, Gng2, Gng12
Regulators	Rgs2, Rgs4, Rgs5, Rgs16
Secondary transducers	FYN, Itpkc, MAPK8ip3
Nuclear effectors	Creb1, Creb3, Creb5

FIGURE 3. **Runx2 controls osteoblast proliferation by modulating the expression of several groups of related genes.** Genes dependent on the growth regulatory C-terminal region of Runx2 were obtained by comparing Affymetrix cDNA expression microarrays. *A,* representative *Runx2* target genes are shown that exhibit a consistent modulation on both day 1 and day 2 in cells expressing wild type Runx2 *versus* Runx2 Δ361 mutant or GFP (*i.e.* control vector). The genes selected here have a greater than 2.4-fold increase or decrease in expression ($p < 0.05$) on either day 1 or 2 (except Gpr54, which was selected as a member of the Gpr family of genes). Comparison of Runx2 wild type (*WT*) *versus* Runx2 Δ361 or wild type *versus* GFP yielded very similar changes in the expression of specific genes. Among the top genes identified in our list are classical bone-specific targets of Runx2 (*e.g.* osteopontin (Spp1), osteocalcin (Bglap2), and matrix metalloproteinase 13 (MMP13)). *B,* functional annotation clustering of 254 genes (>2-fold modulation with wild type Runx2 relative to Runx2 Δ361 at Day 1; $p > 0.05$) was performed using David 2.0 (data base for annotation, visualization, and integrated discovery, available on line). The *pie chart* shows the classification of annotated genes into different biological and cellular categories. *C, Runx2*-dependent genes related to G protein-coupled receptors encode proteins that operate at different steps within a signaling cascade.

genes that are not directly linked to cell growth control. A small set of 12 genes that is significantly modulated by Runx2 Δ361 relative to cells expressing GFP from the empty vector control was excluded from the analysis.

Our analysis revealed strong up-regulation of several well known *Runx2* target genes in osteoblasts including Bone Gla Protein 2/Osteocalcin (*BGP2/OC*), matrix metalloproteinase 13 (*MMP13*), and secreted phosphoprotein/osteopontin (*SPP/OP*) (Fig. 3*A*). Comparison of genes modulated between wild type Runx2 and the Δ361 mutant or wild type Runx2 and GFP (control vector) revealed very similar changes in the expression of specific genes. Interspersed among established target genes for *Runx2*, we observed several other genes that similarly exhibited pronounced changes in expression with the wild type but not the mutant Δ361 protein. These genes include tissue inhibitor of matrix metalloproteinase-3 (*TIMP-3*), procollagen, type VI, α2 (*Col6a2*) and pan-hematopoietic expression (*Phemx*)/tetraspannin 32 (*Tspan32*). Interestingly, *Phemx/Tspan32* is a known target gene for RUNX1/AML1 in hematopoietic cells, whereas distinct members of the *TIMP* and collagen multigene families are *Runx2* target genes in other cells and tissues (46–49). Taken together, our genome-wide expression profiling experiments reveal that the C terminus is required for changes in the expression of known target genes.

To understand which cell functions and regulatory pathways are controlled by the C terminus of Runx2 during cell growth inhibition, we applied functional clustering of genes by gene ontology analysis (*e.g.* David 2.0). We selected 313 Affymetrix probe sets that are expressed at measurable basal levels (arbitrary signal strength above 25), are statistically significant ($p < 0.05$), and exhibit a 2-fold or greater change in expression between the wild type and the mutant Δ361 protein. Of these, 194 probe sets genes are repressed by Runx2, and 119 probe sets exhibited activation. Functional annotation clustering revealed that these 313 probe sets represent at least 254 independent genes that can be grouped into multiple clusters with different biological functions (Fig. 3*B*). We detected modulations in the expression of several osteoblast-related genes (*e.g.* osteocalcin, osteopontin, bone sialoprotein, alkaline phosphatase, collagens, matrix metalloproteinases, and proteoglycans), mRNAs for proteins involved in cell adhesion and cell to cell communication (*e.g.* cadherins and miscellaneous cell surface receptors), as well as a number of genes broadly related to growth factor/cytokine-mediated cell signal-

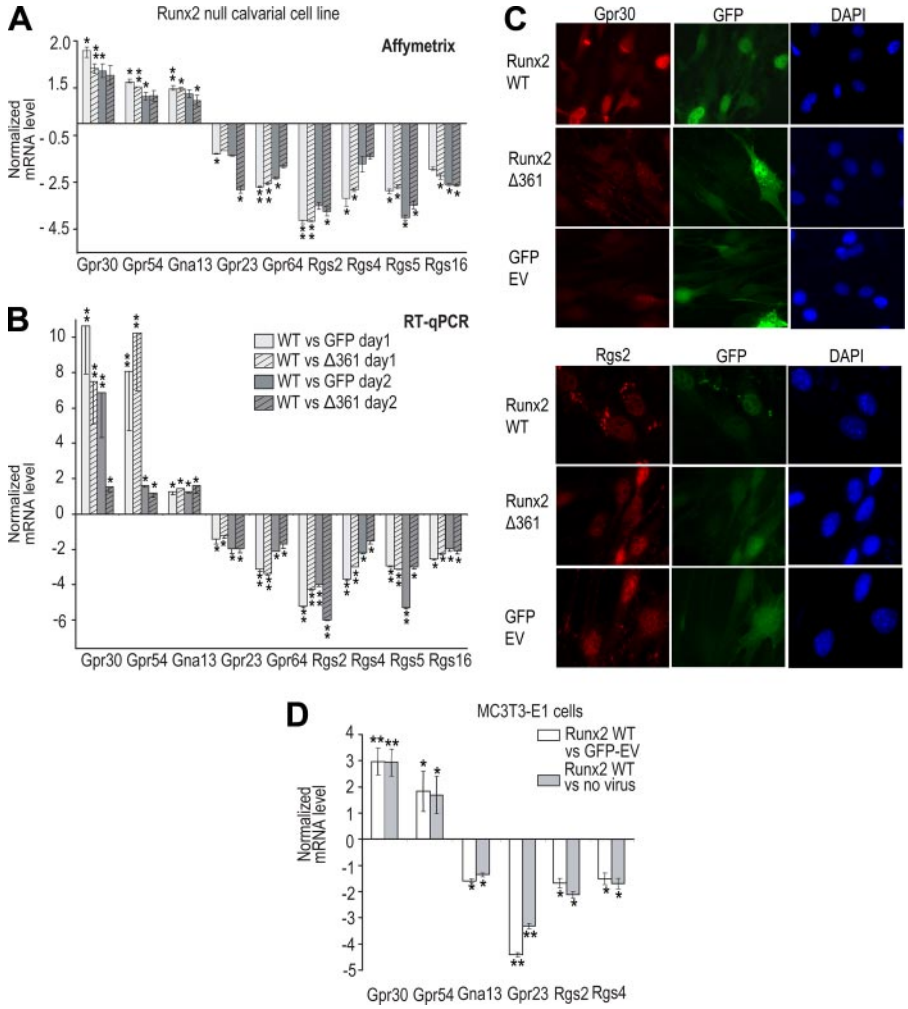

FIGURE 4. **Validation of Runx2-dependent regulation of G protein-coupled receptor signaling components in osteoprogenitors and MC3T3 osteoblasts.** Expression of *Runx2*-dependent genes related to G protein-coupled receptor signaling as determined by Affymetrix microarrays (*A*) using RNA samples obtained from reconstitution assays with *Runx2* null cells (see Figs. 1 and 2) were validated using qRT-PCR analysis (*B*). The mRNA expression levels of cells infected with wild type Runx2 were plotted as fold change relative to cells infected with a vector expressing the Runx2 Δ361 mutant or GFP. *Error bars* reflect standard deviation of Affymetrix values from duplicate independent experiments and qRT-PCR values from triplicate experiments. Gene expression values measured by qRT-PCR were normalized using GAPDH as internal control. Statistical significance of the data was determined by Student's *t* test, and values with $p < 0.05$ are indicated by an *asterisk*, and values with $p < 0.01$ have *two asterisks*. *C, Runx2* null cells were fixed and stained for Gpr30 and Rgs2 immunofluorescence upon infection with adenovirus expressing wild type Runx2, Δ361 mutant, or GFP (control vector). Wild type Runx2 modestly reduces Rgs2 protein level in the nucleus, albeit that Rgs2 detection is evident at bright aggregates in the cytoplasm. *DAPI*, 4′,6-diamidino-2-phenylindole. *D,* forced expression of Runx2 upon adenoviral infection in MC3T3 cells modulates the endogenous mRNA levels of the indicated genes as determined by qRT-PCR at day 1 after infection. The mRNA levels of GPCR-related genes in cells expressing wild type Runx2 were plotted as fold change over GFP and no virus controls and normalized using GAPDH as internal control. Statistical significance of the data was determined by Student's *t* test, and values with $p < 0.05$ are indicated by *one asterisk*, and values with $p < 0.01$ have *two asterisks*.

ing. Strikingly, of the 254 genes we identified, 33 genes (~13%) represent ligands, receptors, G proteins, regulators, second messengers, or nuclear effectors of GPCR-signaling pathways (Fig. 3*C*). Because many G protein-signaling pathways are functionally linked to control of cell proliferation, it is plausible that Runx2 may suppress cell proliferation at least in part by modulating the sensitivity of selected G protein-coupled receptor signaling pathways.

Runx2 Regulates Components of G Protein-coupled Signaling in Osteoblast Progenitors—Among the targets of the full-length Runx2 protein, we identified four genes that encode regulators of G protein signaling (RGS) proteins (*i.e. RGS-2, -4, -5,* and *-16*), as well as five genes encoding G proteins (*i.e. Gna13*) or G protein-coupled receptors (*i.e. Gpr23, Gpr30, Gpr54,* and *Gpr64*). The four RGS genes represent members of the R4-subfamily of proteins, whereas the other five genes encode a more diverse set of proteins that are linked to signaling events involving cyclic AMP, steroid hormone biology, and/or phospholipids. This set of nine genes that we collectively refer to as the "GPCR gene panel" is of particular interest, because of extensive conceptual links between GPCR signaling and processes controlling cell proliferation (50). Furthermore, several genes in this panel were consistently and reproducibly detected (*i.e.* two or more times within the same microarray, in each of the Affymetrix microarray replicates and/or on two different days) and exhibited a statistically robust modulation ($p < 0.05$) in expression upon introduction of Runx2.

We used qRT-PCR analysis to validate changes in the expression levels of the GPCR panel of genes as detected by Affymetrix analysis (Fig. 4, *A* and *B*). The results show that qualitative changes in gene expression observed by Affymetrix analysis are also observed by qRT-PCR analysis. However, qRT-PCR analysis consistently equaled or exceeded values measured by Affymetrix analysis. Strikingly, the qPCR data show that *Gpr30* and *Gpr54* are strongly up-regulated at day 1 (up to 6–10-fold), whereas *Gna13* is only modestly up-regulated (~1.5-fold) (Fig. 4, *A* and *B*). For comparison, the four Rgs genes (*i.e. Rgs-2, -4, -5,* and *-16*), as well as *Gpr23* and *Gpr64* are each down-regulated in the presence of Runx2 by 2–6-fold. Expression of this subset of six genes is modulated by Runx2 at both days we analyzed (day 1 and day 2). Thus, our data show selective changes in the expression of several G protein signaling-related genes that are either stimulated or inhibited by Runx2.

We validated changes in expression of two of these genes, *Gpr30* and *Rgs2*, at the protein level by *in situ* immunofluorescence in *Runx2* null cells. Gpr30 protein expression is below the level of detection in the absence of Runx2 or in the presence of

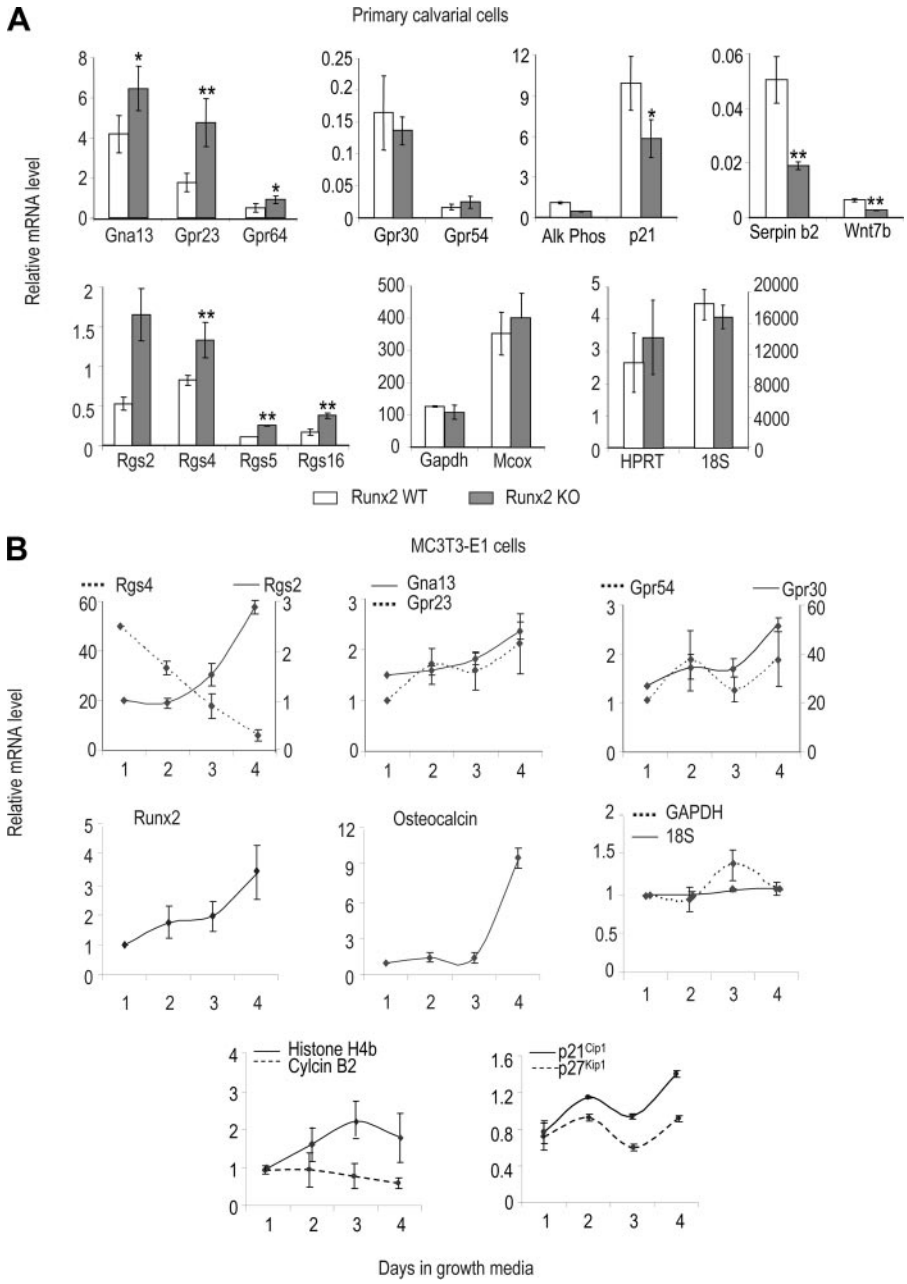

FIGURE 5. **Expression of G protein-coupled receptor signaling components at distinct biological stages of osteogenic differentiation.** *A,* expression of *Runx2*-dependent genes related to G protein-coupled receptor signaling and other markers was examined by qRT-PCR in mesenchymal progenitor cells obtained from the calvarial regions of Runx2 wild type and *Runx2* null (*KO*) mice at embryonic day 17.5 and maintained in subconfluent culture for three passages. Several housekeeping genes were used as internal controls to validate differences in mRNA levels (*Gapdh, Mcox, rRNA,* and *Hprt*). mRNA levels of all different genes were plotted as fold change relative to each other (Gpr64 expression in Runx2 KO cells was arbitrary set as 1). *Error bars* represent standard error between four different mRNA preparations, each derived from multiple mouse embryos. Statistical significance of the data was determined by Student's *t* test, and values with $p < 0.05$ are indicated by *one asterisk*, and values with $p < 0.01$ have *two asterisks*. *B,* expression of representative GPCR-related genes, as well as *Runx2* and bone phenotypic genes, was monitored by qRT-PCR analysis during growth of MC3T3 osteoblasts. MC3T3 cells were grown in proliferating media for 4 days until confluency. The levels for each mRNA were plotted relative to day 1 and normalized by 18 S rRNA as internal control. *Error bars* represent mean ± S.E. between three independent plates.

the Δ361 mutant protein, but it is clearly detectable upon induction by wild type Runx2 (Fig. 4*C*), consistent with RNA expression data (Fig. 4*B*). Similarly, Rgs2 protein expression is detectable in the absence of Runx2, but decreased upon expression of wild type Runx2 (Fig. 4*C*).

To address whether these Runx2-dependent genes are also modulated by Runx2 in committed pre-osteoblasts that endogenously express Runx2 at low levels, we examined the expression of our GPCR gene panel in MC3T3 cells infected with adenoviral vectors expressing Runx2 (and GFP) or the corresponding empty vector that expresses only GFP. Corroborating the data we obtained in *Runx2* null cells (Fig. 4, *A* and *B*), expression of *Gpr30* and *Gpr54* is enhanced, and expression of *Gpr23*, *Rgs2* and *Rgs4* is down-regulated (Fig. 4*D*). Expression of *Gpr64, Rgs5,* and *Rgs16* is below the level of detection in MC3T3 osteoblasts, indicating differences in the expression of these GPCR-related genes in osteogenic progenitors and committed osteoblasts (see below). The only gene that exhibited opposite changes in expression upon elevation of *Runx2* is the gene for the Gα13 protein (*Gna13*); *Gna13* expression is enhanced in *Runx2* null cells but down-regulated in MC3T3 osteoblasts (Fig. 4*D*). Hence, although many *Runx2*-responsive genes are consistently up- or down-regulated, individual genes may be differently regulated by Runx2 depending on the cell type or stage of lineage commitment.

Selective Expression of Runx2-dependent Genes Encoding Factors Involved in G Protein Signaling during Different Stages of Osteoblast Phenotype Maturation—Studies from our group and others suggest that Runx2 mediates lineage commitment of osteoprogenitors, as well as controls the proliferative expansion of pre-osteoblasts and subsequent maturation of quiescent pre-osteoblastic cells into mature osteoblasts. To understand the physiological role that genes involved in G protein signaling play in control of osteoblast growth by Runx2, we examined expression of the Runx2-dependent GPCR gene panel in two different cell culture models that reflect key stages of osteoblast lineage progression (Fig. 5).

We first compared expression profiles of our selected gene set in primary calvarial osteoprogenitors expressing normal

wild type Runx2 that can be induced to differentiate into mature osteoblasts and primary *Runx2* null cells that are phenotype-arrested and exhibit a more immature mesenchymal progenitor phenotype. To investigate which genes of the GPCR panel are expressed in either of these two stages of osteogenic differentiation, we determined their mRNA levels by qRT-PCR (Fig. 5*A*). We found that 7 of 9 genes analyzed are expressed at significantly lower levels in primary calvarial osteoblasts from wild type mice than in pre-osteoblastic progenitors that lack Runx2. For comparison, several osteoblast related genes (*e.g.* alkaline phosphatase (*Alk Phos*), *Wnt7B, Serpinb2,* and the Cdk inhibitor *p21*) are more prominently expressed in calvarial osteoblasts, whereas a series of housekeeping genes does not show appreciable changes in expression (*e.g.* glyceraldehyde-3-phosphate dehydrogenase (*Gapdh*), 18 S rRNA, mitochondrial cytochrome oxidase (*Mcox*), and hypoxanthine-phosphoribosyltransferase (*Hprt*)) (Fig. 5*A*). Because *Runx2* null calvarial cells are less mature than calvarial osteoblast, the results suggest that the GPCR genes are preferentially expressed at elevated levels at the early stages of osteogenic lineage commitment.

The expression of two other Runx2-responsive genes (*Gpr30* and *Gpr54*) we identified in complementation assays with *Runx2* null cells is not significantly different between primary calvarial osteoblasts from Runx2 wild type or *Runx2* null mice. One plausible explanation of these data is that short term forced expression of Runx2 in *Runx2* null cells will yield an acute response, whereas calvarial cells with a *Runx2* null phenotype may have undergone long -term adaptation (during fetal development) perhaps by invoking compensatory mechanisms that bypass a dependence on regulation by Runx2.

We subsequently assessed how G protein signaling-related genes are controlled during the switch from active proliferation to density inhibition of osteoblast growth. To reduce contributions of differentiation-related processes, these experiments were performed in subconfluent cultures in nondifferentiating medium lacking exogenous agents that expedite osteoblast maturation (*e.g.* absence of ascorbic acid and β-glycerol phosphate). Based on our experience, MC3T3-E1 cells achieve maximum proliferation (monitored by FACS analysis) between days 2 and 3 after plating, with contact inhibition of cell growth occurring around day 4 (5, 6). Accordingly, there is a slight decline in histone H4 mRNA levels and a concomitant increase in expression of the Cdk inhibitors p21 and p27 at day 4 after plating (Fig. 5*B*).

Runx2 mRNA expression increases throughout the 4-day culturing period (Fig. 5*B*), consistent with previous findings (6). Under our experimental conditions, osteocalcin mRNA is 4-fold enhanced above a minimal level that is evident at the three earlier days. The results show that *Rgs2* and *Rgs4* are reciprocally regulated with *Rgs4* diminishing and *Rgs2* increasing as the proliferative potential of cells decreases by day 4 (Fig. 5*B*). Similar results were obtained during osteoblast differentiation using osteogenic conditions (data not shown). In contrast, expression of *Gpr23*, *Gpr30*, *Gpr54,* and *Gna13* does not change appreciably but tends to increase by day 4 (Fig. 5*B*). Our data indicate that cessation of proliferation correlates with loss of *Rgs4* and stimulation of *Rgs2*, whereas expression of the other

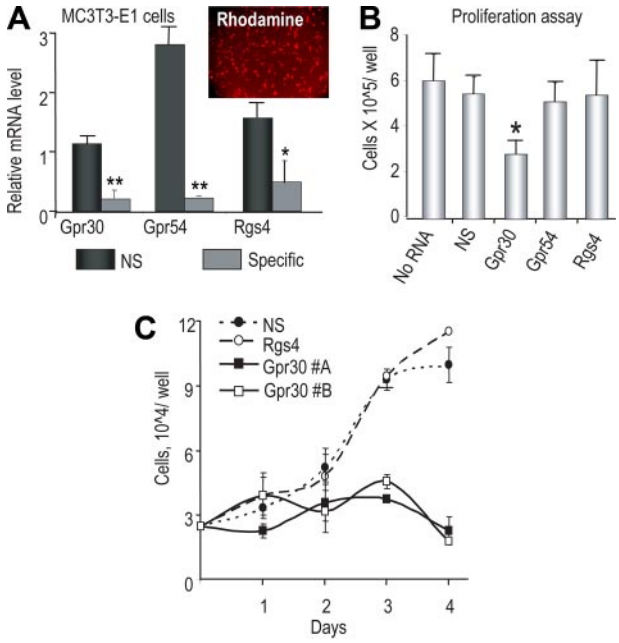

FIGURE 6. **GPR30 regulates proliferation of MC3T3 osteoblasts.** MC3T3 cells were transfected with siRNAs (50 nM each) for Gpr30, Gpr54, Rgs4, or nonsilencing (*NS*) siRNA control in semi-confluent cultures and replated in a 1:3 ratio 24 h after transfection. Following a 36-h culture period, the subconfluent cell population was trypsinized, and cells were counted and harvested for RNA analysis. *A,* efficacy of each siRNA to knock down target gene expression was estimated by qPCR analysis. Levels of mRNA were plotted relative to RNA samples from untransfected control cells. *Error bars* represent standard error between two different RNA samples. Statistical significance of the data was determined by Student's *t* test, and values with $p < 0.05$ are indicated by *one asterisk*, and values with $p < 0.01$ have *two asterisks*. The efficiency of siRNA transfection was monitored using rhodamine-labeled control siRNA signal. *B,* biological effects of distinct siRNAs on proliferation of MC3T3 osteoblasts were determined by cell counting at 60 h after initiating siRNA treatment. *Error bars* represent the range of cell counts from triplicate samples. Statistical significance of the data was determined by Student's *t* test, and values with $p < 0.01$ are indicated by an *asterisk*. *C,* growth curves were obtained by cell counting at daily intervals until 4 days after treatment with nonsilencing (*NS*) RNA or siRNAs against Rgs4 or Gpr30 (*#A*, Ambion; *#B,* Dharmacon). Day 0 is the day when siRNA-transfected cells were replated. *Error bars* reflect variation observed in at least three independent measurements.

GPCR-related genes we detected is sustained throughout the culturing period.

One reason for the absence of significant changes in the expression of *Runx2*-responsive genes during osteoblast growth inhibition is that these genes are most likely not solely regulated by Runx2. For example, although Runx2 represses *Rgs2* in *Runx2* null cells, it may attenuate the expression of this gene to counteract excessive activation by another factor during osteoblast growth and differentiation. Similarly, modest elevation of Gpr30 mRNA levels in our time course could be the result of an attenuating factor that is up-regulated in parallel with Runx2-dependent activation of Gpr30.

Runx2-activated Gene Gpr30 Is Required for Proliferation of MC3T3 Osteoblasts—To understand the biological consequences on osteoblast proliferation of Runx2 regulating specific classes of genes, we focused initially on *Gpr30* that stimulates cyclic AMP signaling and is prominently expressed in proliferating osteoblasts. We used a loss-of-function approach and depleted *Gpr30* by siRNA transfection in MC3T3 osteoblasts (Fig. 6). Treatment of cells with siRNA against *Gpr30* but not with control nonsilencing RNA reduces *Gpr30* expression and

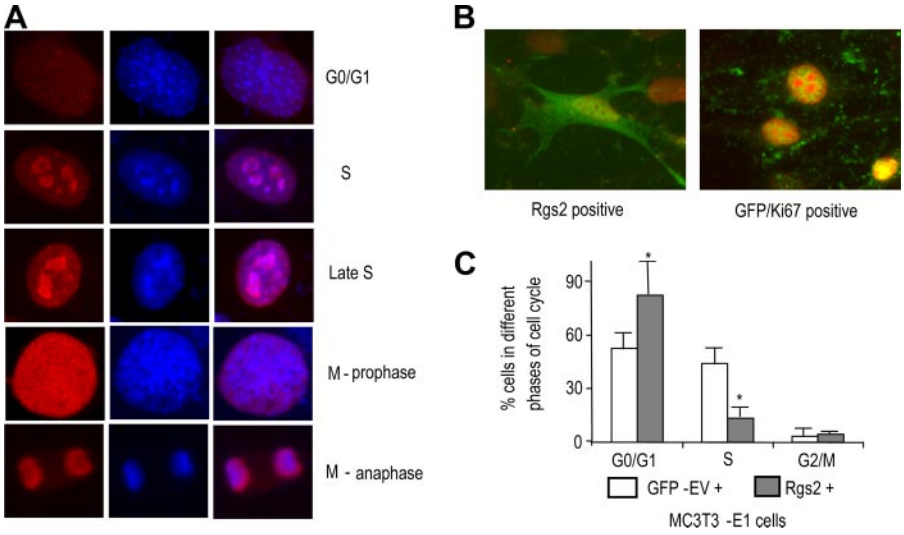

FIGURE 7. **Overexpression of Rgs2 changes cell cycle distribution in MC3T3 osteoblasts.** MC3T3 cells were transfected on coverslips with cytomegalovirus-driven expression vectors for Rgs2 or EGFP as control and fixed 36 h after transfection. Cells were examined by fluorescence microscopy for Ki67 and Rgs2 or GFP to assess the fraction of transfected cells in different cell cycle stages. The number of cells in each phase of the cell cycle was counted separately for both Rgs2 and EGFP-positive cell populations. *A,* representative micrographs of Ki67 immunofluorescence signals in MC3T3 cells. Similar to human Ki67, mouse Ki67 exhibits a cell cycle-related staining pattern that is related in part to dynamic changes in the organization of nucleoli at different stages of cell cycle. *B,* representative immunofluorescence image of MC3T3 cells positive for expression of Rgs2 or GFP. *C,* cell cycle distribution of MC3T3 cells expressing exogenous Rgs2 or GFP. We analyzed 100 cells each for three distinct coverslips (total $n = 300$), and *error bars* represent the range of these triplicate cell counts. Statistical significance of the data was determined by Student's *t* test, and values with $p < 0.01$ are indicated by an *asterisk*.

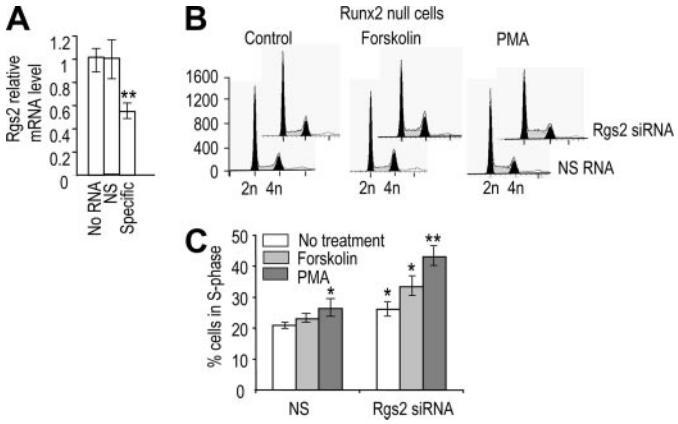

FIGURE 8. **Rgs2 deficiency changes cell cycle distribution in *Runx2* null osteoprogenitor cells.** *Runx2* null cells were transfected with 50 mM each of siRNA to Rgs2 or a nonsilencing (*NS*) siRNA control. Cells were re-plated 24 h after transfection in a 1:3 ratio and 12 h after replating treated with 1 μM PMA, 10 μM forskolin, or DMSO (vehicle control). After 24 h of treatment, cells were collected, and cell cycle distribution was analyzed by propidium iodide staining and FACS analysis. *A,* level of Rgs2 knockdown was monitored by qRT-PCR. *Error bars* represent S.E. between two different samples. The efficiency of siRNA transfection was monitored using a rhodamine-labeled control siRNA to GFP. Statistical significance of the data was determined by Student's *t* test, and values with $p < 0.05$ are indicated by *asterisks*. *B,* cell cycle distribution of *Runx2* null cells treated with either siRNA for Rgs2 or nonsilencing RNA in the presence or absence of PMA (1 μM) or forskolin (10 μM) was established by FACS analysis. *C,* quantitation of the percentage of cells in S phase based on FACS data. Statistical significance of the data was determined by Student's *t* test, and values with $p < 0.05$ are indicated by *asterisks*, and values with $p < 0.01$ have *two asterisks*.

inhibits cell proliferation (Fig. 6). Parallel experiments using specific siRNAs against *Gpr54* and *Rgs4*, which are both co-expressed with *Gpr30* in proliferating osteoblasts, show the expected reductions in gene expression but did not reveal siRNA-mediated changes in cell number (Fig. 6). Furthermore, combined treatment of *Gpr30* and *Gpr54* siRNA or any other combination of siRNAs for GPCR-related proteins does not magnify cell growth inhibition caused by reducing *Gpr30* alone (data not shown). Taken together, our data indicate that although the majority of GPCR-related proteins are not rate-limiting under standard cell culture conditions, the *Runx2*-activated gene *Gpr30* stimulates proliferation of MC3T3 osteoblasts.

Runx2-repressed Gene Rgs2 Attenuates Proliferation of Runx2 Null Osteoprogenitors and Lineage-committed MC3T3 Osteoblasts—Unlike the Runx2-activated gene *Gpr30*, which is an agonist for cAMP signaling, *Rgs2* attenuates this pathway. The function of *Rgs2*, which is repressed by Runx2, was examined by elevating its low levels in proliferating MC3T3 osteoblasts by forced expression (Fig. 7). The effect of up-regulating *Rgs2* expression levels in MC3T3 osteoblasts on cell cycle progression was measured using immunofluorescence microscopy with Ki67 antibodies (Fig. 7). Ki67 is a microscopic marker that permits assessment of the cell cycle stage of individual cells, and the subnuclear localization of Ki67 is related to nucleolar reorganization. For example, the Ki67 pattern in osteoblasts changes from a micropunctate pattern that is evident in G_1 phase cells to a focal organization that becomes successively more prominent as cells progress through S and G_2 phases (Fig. 7*A*). In parallel, we transfected cells with expression vectors for RGS2 or GFP. Fluorescence visualization of RGS2 or GFP in cells reveals which cells have high levels of either protein (Fig. 7*B*). In transfected cells that exogenously express *Rgs2*, there are more G_1 cells and less S phase based on the cell cycle stage-specific staining patterns of Ki67 (Fig. 7) compared with cells that express GFP. Thus, these data indicate at the single-cell level that RGS2 inhibits cell growth of MC3T3 osteoblasts under basal (*i.e.* un-induced) conditions.

To corroborate the conclusion that *Rgs2* is a key attenuator of osteoblast proliferation, we performed RNA interference experiments. *Rgs2* expression is normally suppressed by Runx2 (see Fig. 4), and *Rgs2* expression is increased in *Runx2* null osteoprogenitors compared with wild type calvarial cells (see Fig. 5*A*). Treatment of *Runx2* null cells with siRNA for *Rgs2* counteracts this elevation in *Rgs2* levels (Fig. 8). *Rgs2* siRNA but not nonsilencing siRNA reduces mRNA levels by at least 2-fold (Fig. 8*A*). Cells were also co-treated with forskolin or phorbol myristate acetate (PMA), each of which stimulates cell cycle progression. Treatment with either agent promotes the inhibitory activity of Rgs2 (51), and thus the effect of Rgs2 siRNA is

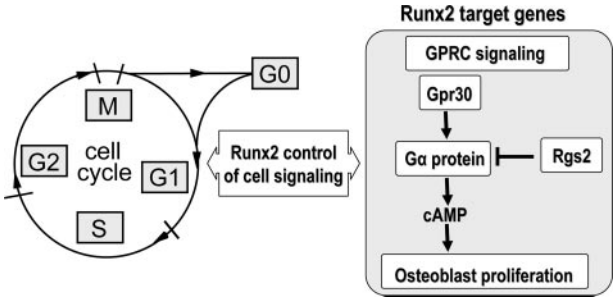

FIGURE 9. **Model for the reciprocal regulatory relationship between osteoblast proliferation and Runx2 control of gene expression.** Runx2 levels are modulated during the cell cycle and are maximal in G_1. We propose that Runx2 controls responsiveness of osteoblasts to mitogenic cues by altering the levels of components for multiple G protein-coupled receptor signaling pathways. In one of the pathways that is depicted here, Runx2 activates expression of Gpr30 and represses Rgs2. The net effect of these modulations is sensitization of cAMP/PKA signaling.

expected to be more prominent. Flow cytometry results show that *Rgs2* siRNA increases the percentage of S phase cells in all treatment groups, and more overtly in cells treated forskolin or PMA (Fig. 8, *B* and *C*). We conclude that the *Runx2*-dependent gene *Rgs2* reduces the mitogenic response of *Runx2* null osteoprogenitor cells. In addition, because Runx2 regulates *Gpr30* and *Rgs2*, and because the activities of Gpr30, Rgs2 and Runx2 proteins are all linked to cAMP levels in osteoblasts (52–54), we propose that Runx2 may regulate cAMP-related signaling pathways to influence osteoblast proliferation (Fig. 9).

DISCUSSION

In this study, we have characterized mechanisms that account for the ability of Runx2 to control osteoblast proliferation using an integrated strategy in which we investigated, first, what functions of Runx2 are required for cell growth control and, second, what downstream targets mediate its growth regulatory function. Using complementation assays where wild type and mutant Runx2 proteins are reintroduced into *Runx2* null calvarial cells, we established that neither TGFβ/BMP2-SMAD-Runx2 nor WW domain signaling (*e.g.* WWOX, SRC/YES-YAP) was required for growth regulatory effects in osteogenic cells. However, DNA binding and C-terminal transcriptional functions of Runx2 are essential for cell growth inhibition, emphasizing the importance of gene expression programs that respond to modulations in Runx2 levels.

We have advanced the idea that Runx2 may control commitment for cell proliferation or osteogenic lineage progression by regulating the integrated cellular response to hormonal and mitogenic stimuli through modulation of the levels of key regulatory proteins that participate in diverse signaling pathways. Because Runx2 attenuates osteoblast proliferation, this factor may directly activate the expression of cell cycle inhibitory proteins or repress mitogenic proteins. Affymetrix gene expression profiling upon expression of either wild type or mutant Runx2 proteins revealed more than 250 genes that are either repressed or activated by wild type Runx2 during cell growth suppression. One striking finding of these studies is that Runx2 coordinately controls multiple components of G protein-coupled receptor (GPCR) signaling in osteoblasts.

GPCRs are prominently expressed in bone and mediate responses to a broad range of physiological stimuli, including growth factors, neurotransmitters, cytokines/chemokines, and peptide hormones (*e.g.* PTH and PTH-related peptide), as well as steroid hormones (*e.g.* estrogen and glucocorticoids) and calcium ion signaling (32, 51, 55–59). For example, our data show that Runx2 controls expression of several G protein-coupled receptors (*e.g.* Gpr30, Gpr54, Gpr23, and Gpr64), regulators of G protein signaling (*e.g.* Rgs2, Rgs4, Rgs5, and Rgs16), and G-α proteins (*e.g.* Gna13). GPCR signaling is functionally linked to control of cell proliferation, because many growth factors signal through small G proteins and many GPCR pathways signal through kinases (*e.g.* PKA, PKC, I3P, and mitogen-activated protein kinases) that actively regulate cell cycle progression. Our study shows that at least two of the nine *Runx2* responsive genes we characterized (*i.e. Gpr30* and *Rgs2*), which have previously been linked to PKA signaling, have functional roles in control of osteoblast proliferation.

Previous studies have shown that Gpr30, which is the non-genomic estrogen receptor (60), promotes or inhibits cell proliferation depending on the presence and type of ligand, the cell type, and the hormonal context (61–65). Expression of Gpr30 is evident in the growth plate in both hypotrophic and quiescent chondrocytes but not in the proliferating region (66), suggesting that its function in chondrocytes is metabolic rather than developmental. We show that Gpr30 is expressed in proliferating osteoblasts, although its level increases by at most 2-fold in post-proliferative osteoblasts. Also, *Gpr30* regulates epidermal growth factor release and can both induce and inhibit activity of mitogen-activated protein kinases (62–66). Our findings establish that *Gpr30* is a *Runx2*-responsive gene and is required for osteoblast proliferation.

The G protein regulator Rgs2 modulates signaling from the PTH/PTH-related peptide receptor in osteoblasts and chondrocytes, as well as permits switching between $G\alpha_s$ and $G\alpha_q$ signaling pathways that stimulate PKC and PKA activity. Previous results have indicated that the *Rgs2* gene promoter is activated by Runx2 (67), but our data clearly indicate that expression of Rgs2, as well as other Rgs proteins, is coordinately down-regulated by Runx2 under our experimental conditions. Forced expression of Rgs2 impedes progression through the cell cycle in G_1 in uninduced osteoblast progenitors, whereas Rgs2 depletion using siRNA increases the proliferative response upon stimulation of PKC (with PMA) or PKA (with forskolin); both PMA and forskolin promote the inhibitory function of Rgs2 (11). Our results indicate that Rgs2, like GPR30, is also a Runx2-dependent regulator of osteoblast growth.

The functions of *Gpr30* and *Rgs2* have been linked to cAMP stimulation of PKA. The resulting activation of cAMP-responsive element-binding protein (CREB) and subsequent CREB-dependent expression of A- and D-type cyclins promotes cell cycle progression through induction of Cdk activity (68–70). We note that at least three CREB proteins (CREB1, CREB3, and CREB5) are also Runx2-responsive (see Fig. 3*C*), consistent with the concept that Runx2 may control a putative growth stimulatory Gpr30-Rgs2-cAMP-PKA-CREB-cyclin-Cdk circuit in osteoblasts.

Our results show that Runx2 stimulates the pro-mitogenic function of *Gpr30* in osteoblasts by enhancing expression of the

Gpr30 gene. Runx2 inhibits the anti-proliferative activity of *Rgs2* by repressing *Rgs2* mRNA expression. The observation that Runx2 activates *Gpr30* and suppresses *Rgs2* to promote cell proliferation is somewhat surprising considering that these genes were identified in our screen designed to define Runx2-dependent growth-suppressive pathways. Apparently, Runx2 is both pro- and anti-proliferative within the same cell type. Several other findings on Runx2 may illuminate this paradox. First, Runx2 has been characterized as a c-*Myc* cooperating oncogene in T cell lymphoma (16, 71), and *Runx2* expression is frequently elevated in osteosarcoma (6)[6] clearly suggesting that Runx2 may have pro-mitogenic functions apart from growth suppressive activities. Furthermore, our other studies suggest that Runx2 is up-regulated by mitogens in osteoblasts during early G_1 where it may have a positive role in cell proliferation (21). For example, osteoblasts express the Cdk inhibitor p21 (72); Runx2 represses *p21* transcription (34), and decreased levels of p21 would promote cell cycle progression by increasing Cdk activity. Runx2 is only down-regulated in late G_1 when cells have committed to a new round of cell division (6, 20). These previous findings indicate that the growth-suppressive function of Runx2 operates during and beyond late G_1, and there may be an obligatory requirement to reduce its protein levels prior to the onset of S phase. Therefore, it is plausible that control of osteoblast growth by Runx2 is cell cycle stage-specific; Runx2 may be pro-mitogenic in early G_1 and anti-mitogenic in late G_1.

This proposed bi-functional role of Runx2 may be analogous to that of c-Myc; c-Myc is pro-mitogenic as an early response factor to growth factor stimulation, but oncogenic activation of c-Myc can trigger the growth-suppressive $p14/p19^{ARF}$ pathway. Similarly, the pro-mitogenic up-regulation of Gpr30 and down-regulation of Rgs2 by Runx2 in mesenchymal cells may be temporally distinct from the ability of Runx2 to control the $p14/p19^{ARF}$ pathway to inhibit cell growth (10, 11). Further studies on the biological bi-functionality of Runx2 during the cell cycle are warranted.

Upon our initial demonstration that *Runx2* null osteoprogenitors proliferate robustly compared with wild type calvarial osteoblasts (5), and the subsequent demonstration that Runx2 levels oscillate during the cell cycle (6, 20), a major focus of our research group has been the identification of cellular programs that are controlled by Runx2 in proliferating cells. Our recent studies have shown that Runx2 controls rRNA transcription thereby modulating protein synthesis (7). Furthermore, loss of Runx2 results in a bypass of senescence and is pre-tumorigenic by increasing the accumulation of DNA damage and formation of phospho-H2A.X foci (10, 11), consistent with the idea that elevation of Runx2 is functionally linked to acquisition of a non-proliferative state in osteoblasts. The finding that Runx2 controls at least two genes (*Gpr30* and *Rgs2*) that are linked to cAMP signaling, as well as a large group of other proteins related to G protein-coupled receptor signaling, indicates that Runx2 modulates the integration of biological information from multiple G protein signaling networks.

The results from this study suggest that Runx2 is a principal regulator of the biological response of osteoblasts to external cues in the bone micro-environment and that Runx2 both sensitizes and desensitizes mitogenic pathways that determine competency for cell cycle progression and osteoblastic lineage commitment. Our studies have several interesting clinical ramifications. First, because Runx2 expression and activity are regulated by estrogen (2), it is possible that the bone-anabolic effects of estrogen and related compounds may occur via a positive feed-forward pathway (estrogen-Runx2-Gpr30-cAMP) that promotes osteoblast proliferation. Furthermore, our results suggest that the beneficial bone-anabolic effects of intermittent PTH administration (51, 59, 73, 74), which has been associated with modulations in Runx2 levels (75), may be biologically linked to Runx2 and cAMP-dependent control of osteoblast proliferation.

Acknowledgments—We thank all members of our research group, especially Mohammad Hassan, Jonathan Gordon, Sayyed Kaleem Zaidi, Anurag Gupta, Ying Zhang, Jason Dobson, Dana Frederick, Sandhya Pande, Yang Lou, Tripti Gaur, and Margaretha van der Deen for reagents, experimental guidance, and/or stimulating discussions. We thank Karen Blyth (University of Glasgow, UK), Linda van Aelst (Cold Spring Harbor Laboratories), and Jennifer Westendorf (Mayo Clinic) for critically reading the manuscript. We also thank Judy Rask for assistance with the preparation of our manuscript.

REFERENCES

1. Lian, J. B., Stein, G. S., Javed, A., van Wijnen, A. J., Stein, J. L., Montecino, M., Hassan, M. Q., Gaur, T., Lengner, C. J., and Young, D. W. (2006) *Rev. Endocr. Metab. Disord.* **7,** 1–16
2. Komori, T. (2008) *Front. Biosci.* **13,** 898–903
3. Blyth, K., Cameron, E. R., and Neil, J. C. (2005) *Nat. Rev. Cancer* **5,** 376–387
4. van Wijnen, A. J., Stein, G. S., Gergen, J. P., Groner, Y., Hiebert, S. W., Ito, Y., Liu, P., Neil, J. C., Ohki, M., and Speck, N. (2004) *Oncogene* **23,** 4209–4210
5. Pratap, J., Galindo, M., Zaidi, S. K., Vradii, D., Bhat, B. M., Robinson, J. A., Choi, J.-Y., Komori, T., Stein, J. L., Lian, J. B., Stein, G. S., and van Wijnen, A. J. (2003) *Cancer Res.* **63,** 5357–5362
6. Galindo, M., Pratap, J., Young, D. W., Hovhannisyan, H., Im, H. J., Choi, J. Y., Lian, J. B., Stein, J. L., Stein, G. S., and van Wijnen, A. J. (2005) *J. Biol. Chem.* **280,** 20274–20285
7. Young, D. W., Hassan, M. Q., Pratap, J., Galindo, M., Zaidi, S. K., Lee, S. H., Yang, X., Xie, R., Javed, A., Underwood, J. M., Furcinitti, P., Imbalzano, A. N., Penman, S., Nickerson, J. A., Montecino, M. A., Lian, J. B., Stein, J. L., van Wijnen, A. J., and Stein, G. S. (2007) *Nature* **445,** 442–446
8. Young, D. W., Hassan, M. Q., Yang, X.-Q., Galindo, M., Javed, A., Zaidi, S. K., Furcinitti, P., Lapointe, D., Montecino, M., Lian, J. B., Stein, J. L., van Wijnen, A. J., and Stein, G. S. (2007) *Proc. Natl. Acad. Sci. U. S. A.* **104,** 3189–3194
9. Zaidi, S. K., Sullivan, A. J., Medina, R., Ito, Y., van Wijnen, A. J., Stein, J. L., Lian, J. B., and Stein, G. S. (2004) *EMBO J.* **23,** 790–799
10. Zaidi, S. K., Pande, S., Pratap, J., Gaur, T., Grigoriu, S., Ali, S. A., Stein, J. L., Lian, J. B., van Wijnen, A. J., and Stein, G. S. (2007) *Proc. Natl. Acad. Sci. U. S. A.* **104,** 19861–19866
11. Kilbey, A., Blyth, K., Wotton, S., Terry, A., Jenkins, A., Bell, M., Hanlon, L., Cameron, E. R., and Neil, J. C. (2007) *Cancer Res.* **67,** 11263–11271
12. Thomas, D. M., Johnson, S. A., Sims, N. A., Trivett, M. K., Slavin, J. L., Rubin, B. P., Waring, P., McArthur, G. A., Walkley, C. R., Holloway, A. J., Diyagama, D., Grim, J. E., Clurman, B. E., Bowtell, D. D., Lee, J. S., Gutierrez, G. M., Piscopo, D. M., Carty, S. A., and Hinds, P. W. (2004) *J. Cell Biol.* **167,** 925–934

[6] N. Teplyuk, G. Stein, and A. van Wijnen, unpublished data.

13. Hinoi, E., Bialek, P., Chen, Y. T., Rached, M. T., Groner, Y., Behringer, R. R., Ornitz, D. M., and Karsenty, G. (2006) *Genes Dev.* **20,** 2937–2942
14. Inman, C. K., and Shore, P. (2003) *J. Biol. Chem.* **278,** 48684–48689
15. Qiao, M., Shapiro, P., Fosbrink, M., Rus, H., Kumar, R., and Passaniti, A. (2006) *J. Biol. Chem.* **281,** 7118–7128
16. Stewart, M., Mackay, N., Hanlon, L., Blyth, K., Scobie, L., Cameron, E., and Neil, J. C. (2007) *Cancer Res.* **67,** 5126–5133
17. Blyth, K., Vaillant, F., Hanlon, L., Mackay, N., Bell, M., Jenkins, A., Neil, J. C., and Cameron, E. R. (2006) *Cancer Res.* **66,** 2195–2201
18. Pratap, J., Lian, J. B., Javed, A., Barnes, G. L., van Wijnen, A. J., Stein, J. L., and Stein, G. S. (2006) *Cancer Metastasis Rev.* **25,** 589–600
19. Vaillant, F., Blyth, K., Andrew, L., Neil, J. C., and Cameron, E. R. (2002) *J. Immunol.* **169,** 2866–2874
20. Galindo, M., Kahler, R. A., Teplyuk, N. M., Stein, J. L., Lian, J. B., Stein, G. S., Westendorf, J. J., and van Wijnen, A. J. (2007) *J. Mol. Hist.* **38,** 501–506
21. Galindo, M., Teplyuk, N., Yang, X., Young, D. W., Javed, A., Lian, J. B., Stein, J. L., Stein, G. S., and van Wijnen, A. J. (2006) *J. Bone Miner. Res.* **21,** S384 (abstr.)
22. Rajgopal, A., Young, D. W., Mujeeb, K. A., Stein, J. L., Lian, J. B., van Wijnen, A. J., and Stein, G. S. (2007) *J. Cell. Biochem.* **100,** 1509–1517
23. Shen, R., Wang, X., Drissi, H., Liu, F., O'Keefe, R. J., and Chen, D. (2006) *J. Biol. Chem.* **281,** 16347–16353
24. Kim, H. J., Kim, J. H., Bae, S. C., Choi, J. Y., Kim, H. J., and Ryoo, H. M. (2003) *J. Biol. Chem.* **278,** 319–326
25. Guenou, H., Kaabeche, K., Mee, S. L., and Marie, P. J. (2005) *Hum. Mol. Genet.* **14,** 1429–1439
26. Marie, P. J. (2003) *Gene* (*Amst.*) **316,** 23–32
27. Balint, E., Lapointe, D., Drissi, H., van der Meijden, C., Young, D. W., van Wijnen, A. J., Stein, J. L., Stein, G. S., and Lian, J. B. (2003) *J. Cell. Biochem.* **89,** 401–426
28. Lee, M. H., Kim, Y. J., Yoon, W. J., Kim, J. I., Kim, B. G., Hwang, Y. S., Wozney, J. M., Chi, X. Z., Bae, S. C., Choi, K. Y., Cho, J. Y., Choi, J. Y., and Ryoo, H. M. (2005) *J. Biol. Chem.* **280,** 35579–35587
29. Kang, J. S., Alliston, T., Delston, R., and Derynck, R. (2005) *EMBO J.* **24,** 2543–2555
30. Bae, J. S., Gutierrez, S., Narla, R., Pratap, J., Devados, R., van Wijnen, A. J., Stein, J. L., Stein, G. S., Lian, J. B., and Javed, A. (2007) *J. Cell. Biochem.* **100,** 434–449
31. Javed, A., Bae, J. S., Afzal, F., Gutierrez, S., Pratap, J., Zaidi, S. K., Lou, Y., van Wijnen, A. J., Stein, J. L., Stein, G. S., and Lian, J. B. (2008) *J. Biol. Chem.* **283,** 8412–8422
32. Swarthout, J. T., D'Alonzo, R. C., Selvamurugan, N., and Partridge, N. C. (2002) *Gene* (*Amst.*) **282,** 1–17
33. Thomas, D. M., Carty, S. A., Piscopo, D. M., Lee, J. S., Wang, W. F., Forrester, W. C., and Hinds, P. W. (2001) *Mol. Cell* **8,** 303–316
34. Westendorf, J. J., Zaidi, S. K., Cascino, J. E., Kahler, R., van Wijnen, A. J., Lian, J. B., Yoshida, M., Stein, G. S., and Li, X. (2002) *Mol. Cell. Biol.* **22,** 7982–7992
35. Jensen, E. D., Niu, L., Caretti, G., Nicol, S. M., Teplyuk, N., Stein, G. S., Sartorelli, V., van Wijnen, A. J., Fuller-Pace, F. V., and Westendorf, J. J. (2008) *J. Cell. Biochem.* **103,** 1438–1451
36. Jensen, E. D., Schroeder, T. M., Bailey, J., Gopalakrishnan, R., and Westendorf, J. J. (2008) *J. Bone Miner. Res.* **23,** 361–372
37. Javed, A., Guo, B., Hiebert, S., Choi, J.-Y., Green, J., Zhao, S.-C., Osborne, M. A., Stifani, S., Stein, J. L., Lian, J. B., van Wijnen, A. J., and Stein, G. S. (2000) *J. Cell Sci.* **113,** 2221–2231
38. Zaidi, S. K., Young, D. W., Javed, A., Pratap, J., Montecino, M., van, W. A., Lian, J. B., Stein, J. L., and Stein, G. S. (2007) *Nat. Rev. Cancer* **7,** 454–463
39. Zhao, M., Qiao, M., Oyajobi, B. O., Mundy, G. R., and Chen, D. (2003) *J. Biol. Chem.* **278,** 27939–27944
40. Cui, C. B., Cooper, L. F., Yang, X., Karsenty, G., and Aukhil, I. (2003) *Mol. Cell. Biol.* **23,** 1004–1013
41. Jones, D. C., Wein, M. N., Oukka, M., Hofstaetter, J. G., Glimcher, M. J., and Glimcher, L. H. (2006) *Science* **312,** 1223–1227
42. Zaidi, S. K., Javed, A., Choi, J.-Y., van Wijnen, A. J., Stein, J. L., Lian, J. B., and Stein, G. S. (2001) *J. Cell Sci.* **114,** 3093–3102
43. Gautier, L., Cope, L., Bolstad, B. M., and Irizarry, R. A. (2004) *Bioinformatics* (*Oxf.*) **20,** 307–315
44. Dennis, G., Jr., Sherman, B. T., Hosack, D. A., Yang, J., Gao, W., Lane, H. C., and Lempicki, R. A. (2003) *Genome Biol.* **4,** 3
45. Harrington, K. S., Javed, A., Drissi, H., McNeil, S., Lian, J. B., Stein, J. L., van Wijnen, A. J., Wang, Y.-L., and Stein, G. S. (2002) *J. Cell Sci.* **115,** 4167–4176
46. Bertrand-Philippe, M., Ruddell, R. G., Arthur, M. J., Thomas, J., Mungalsingh, N., and Mann, D. A. (2004) *J. Biol. Chem.* **279,** 24530–24539
47. Harada, Y., Harada, H., Downing, J. R., and Kimura, A. (2001) *Biochem. Biophys. Res. Commun.* **284,** 714–722
48. Selvamurugan, N., and Partridge, N. C. (2000) *Mol. Cell Biol. Res. Commun.* **3,** 218–223
49. Zheng, Q., Zhou, G., Morello, R., Chen, Y., Garcia-Rojas, X., and Lee, B. (2003) *J. Cell Biol.* **162,** 833–842
50. Rozengurt, E. (2007) *J. Cell. Physiol.* **213,** 589–602
51. Kronenberg, H. M. (2006) *Ann. N. Y. Acad. Sci.* **1068,** 1–13
52. Roy, A. A., Nunn, C., Ming, H., Zou, M. X., Penninger, J., Kirshenbaum, L. A., Dixon, S. J., and Chidiac, P. (2006) *J. Biol. Chem.* **281,** 32684–32693
53. Filardo, E. J., Quinn, J. A., Frackelton, A. R., Jr., and Bland, K. I. (2002) *Mol. Endocrinol.* **16,** 70–84
54. Bertaux, K., Broux, O., Chauveau, C., Hardouin, P., Jeanfils, J., and Devedjian, J. C. (2006) *Bone* (*Elmsford*) **38,** 943–950
55. Hsiao, E. C., Boudignon, B. M., Chang, W. C., Bencsik, M., Peng, J., Nguyen, T. D., Manalac, C., Halloran, B. P., Conklin, B. R., and Nissenson, R. A. (2008) *Proc. Natl. Acad. Sci. U. S. A.* **105,** 1209–1214
56. Bodine, P. V., and Komm, B. S. (2006) *Rev. Endocr. Metab Disord.* **7,** 33–39
57. Pi, M., and Quarles, L. D. (2005) *J. Cell. Biochem.* **95,** 1081–1092
58. Dvorak, M. M., and Riccardi, D. (2004) *Cell Calcium* **35,** 249–255
59. Rosen, C. J. (2003) *Crit. Rev. Eukaryotic Gene Expression* **13,** 25–38
60. Carmeci, C., Thompson, D. A., Ring, H. Z., Francke, U., and Weigel, R. J. (1997) *Genomics* **45,** 607–617
61. Prossnitz, E. R., Arterburn, J. B., and Sklar, L. A. (2007) *Mol. Cell. Endocrinol.* **265–266,** 138–142
62. Manavathi, B., and Kumar, R. (2006) *J. Cell. Physiol.* **207,** 594–604
63. Filardo, E. J., and Thomas, P. (2005) *Trends Endocrinol. Metab.* **16,** 362–367
64. Revankar, C. M., Cimino, D. F., Sklar, L. A., Arterburn, J. B., and Prossnitz, E. R. (2005) *Science* **307,** 1625–1630
65. Kanda, N., and Watanabe, S. (2004) *J. Investig. Dermatol.* **123,** 319–328
66. Chagin, A. S., and Savendahl, L. (2007) *J. Clin. Endocrinol. Metab* **92,** 4873–4877
67. Thirunavukkarasu, K., Halladay, D. L., Miles, R. R., Geringer, C. D., and Onyia, J. E. (2002) *J. Cell. Biochem.* **85,** 837–850
68. Beier, F., Ali, Z., Mok, D., Taylor, A. C., Leask, T., Albanese, C., Pestell, R. G., and LuValle, P. (2001) *Mol. Biol. Cell* **12,** 3852–3863
69. D'Amico, M., Hulit, J., Amanatullah, D. F., Zafonte, B. T., Albanese, C., Bouzahzah, B., Fu, M., Augenlicht, L. H., Donehower, L. A., Takemaru, K., Moon, R. T., Davis, R., Lisanti, M. P., Shtutman, M., Zhurinsky, J., Ben-Ze'ev, A., Troussard, A. A., Dedhar, S., and Pestell, R. G. (2000) *J. Biol. Chem.* **275,** 32649–32657
70. Desdouets, C., Matesic, G., Molina, C. A., Foulkes, N. S., Sassone-Corsi, P., Brechot, C., and Sobczak-Thepot, J. (1995) *Mol. Cell. Biol.* **15,** 3301–3309
71. Stewart, M., Terry, A., Hu, M., O'Hara, M., Blyth, K., Baxter, E., Cameron, E., Onions, D. E., and Neil, J. C. (1997) *Proc. Natl. Acad. Sci. U. S. A.* **94,** 8646–8651
72. Drissi, H., Hushka, D., Aslam, F., Nguyen, Q., Buffone, E., Koff, A., van Wijnen, A., Lian, J. B., Stein, J. L., and Stein, G. S. (1999) *Cancer Res.* **59,** 3705–3711
73. Jilka, R. L. (2007) *Bone* (*Elmsford*) **40,** 1434–1446
74. Li, X., Liu, H., Qin, L., Tamasi, J., Bergenstock, M., Shapses, S., Feyen, J. H., Notterman, D. A., and Partridge, N. C. (2007) *J. Biol. Chem.* **282,** 33086–33097
75. Bellido, T., Ali, A. A., Plotkin, L. I., Fu, Q., Gubrij, I., Roberson, P. K., Weinstein, R. S., O'Brien, C. A., Manolagas, S. C., and Jilka, R. L. (2003) *J. Biol. Chem.* **278,** 50259–50272